Carbohydrate Polymers 89 (2012) 1198–1206

Contents lists available at SciVerse ScienceDirect

Carbohydrate Polymers

journal homepage: www.elsevier.com/locate/carbpol

Mechanical properties of calcium alginate fibers produced with a microfluidic device

Teresa R. Cuadros[a,*], Olivier Skurtys[b], José M. Aguilera[a]

[a] Pontificia Universidad Católica de Chile, School of Engineering, Department of Chemical and Bioprocess Engineering, P.O. Box 306, Santiago 22, Chile
[b] Universidad Técnica Federico Santa María, Department of Mechanical Engineering, Av. Vicuña Mackenna 3939, Santiago, Chile

ARTICLE INFO

Article history:
Received 28 September 2011
Received in revised form 12 January 2012
Accepted 29 March 2012
Available online 5 April 2012

Keywords:
Alginate gel
Diffusion
Mechanical properties
Microfluidic
Fibers
Eggs-box model

ABSTRACT

Fibers are important microstructural elements in many foods. The main objective of this research was to produce calcium alginate fibers with uniform diameters (about 300 and 550 μm) using a microfluidic device (MFD) and to study the effect of concentration of sodium alginate [Alg] and calcium chloride [$CaCl_2$] on their mechanical properties (MP). Moisture content (MO) and MP as maximum tensile stress (σ_{max}), tensile strain at break ($\Delta L/L_0$) and apparent Young's modulus (E) of fibers were determined and a statistical model and surface responses were developed as a function of [Alg] and [$CaCl_2$]. As [$CaCl_2$] increased first a strengthening and then a weakening of fibers were observed. Furthermore, σ_{max} increased with the addition of Ca^{2+} and a maximum of σ_{max} was obtained for a [$CaCl_2$] around 1.4% (exceeding several times the stoichiometric requirements of the carboxylate groups of the polymer). Such behavior prompted a molecular explanation of what happens during gelation based on the "egg-box model" and this model is tried to complete. Moreover, fibers with [Alg] ≥1.8% showed high extensibility ($\Delta L/L_0$ around 100%) and low values of MO. High values of E (~0.5 MPa) were obtained for [$CaCl_2$] close to 1.4%. A greater understanding is needed of the interaction between cation-polysaccharide-water, taking into account [Alg] and [$CaCl_2$] to predict the mechanical behavior of fibers. Calcium alginate fibers are important in food engineering as texture and microencapsulation agents.

1. Introduction

Structure formation in food materials is influenced by ingredient properties and processing conditions, including shearing forces. The use of well-defined flows, such as simple shear, turned out to be essential to study and control the structure formation process in fibrous foods (van der Goot, Peifhambardoust, Akkermans, & van Oosten-Manski, 2008). Recently, several microfluidic applications for producing various microstructural elements, such as bubbles, particles, fibers, strips, microcapsules have been reported (Bhattarai, Li, Edmondson, & Zhang, 2006; Fan, Du, Huan, Wang, Wang, & Zhang, 2005; Mikolajczyk & Wolowska-Czapnik, 2005; Shin et al., 2007; Skurtys & Aguilera, 2008a,b; Skurtys, Bouchon, & Aguilera, 2008; Vreeker, Li, Fang, Appelqvist, & Mendes, 2008).

Alginate is a powerful thickening, stabilizing and gel-forming agent used in foods to produce a variety of gel products (cold instant puddings, fruit gels, dessert gels, onion rings, imitation caviar) (Belitz, Grosch, & Schieberle, 2004). In particular, calcium alginate fibers may find applications in the structuring of various food analogs since alginate is an inexpensive and easily available natural biomaterial. Alginate fibers are also currently used to encapsulate flavor, enzymes, proteins, drugs and active components (Bhattarai et al., 2006; Mikolajczyk & Wolowska-Czapnik, 2005; Tonnesen & Karlsen, 2002; Wang, Liu, Gao, Liu, & Tong, 2008). Several methods have been utilized to fabricate alginate fibers with diameters smaller than 100 μm: extruding-spinning achieving fiber diameters of 40–50 μm (Fan et al., 2005); electrospinning of nanofibers such as alginate-PEO(poly-ethylene oxide) fibers with diameters between 20 and 100 nm (Bhattarai et al., 2006), and 40–200 nm (Moon, Ryu, Choi, Jo, & Farris, 2009); spinning machine yielding fiber diameters <80 μm (Mikolajczyk & Wolowska-Czapnik, 2005); and, a microfluidic device (similar to the one in this study) whose fibers have diameters ~20 μm (Shin et al., 2007). However, all these studies lack of a detailed study of the mechanical properties of the resulting fibers.

Alginate belongs to a family of linear copolymers of (1 → 4)-linked β-D-mannuronic acid (M) and α-L guluronic acid (G) residues, with M and G residues present in varying proportions and sequences depending on the alginic acid source. Alginate gelation occurs when divalent cations (usually Ca^{2+}) interact with blocks of G residues. In the dialysis method, calcium ions diffuse into the alginate solution with a rapid, strong and irreversible formation of gel (Draget, Moe, Skjak-Braek, & Smidsrod, 2006). These gels have

* Corresponding author. Tel.: +56 2 3544237; fax: +56 2 3545803.
E-mail addresses: tcuadroc@uc.cl, trcuadro@ing.puc.cl, trcuadros@gmail.com (T.R. Cuadros).

0144-8617/$ – see front matter © 2012 Elsevier Ltd. All rights reserved.
http://dx.doi.org/10.1016/j.carbpol.2012.03.094

the particular feature of being cold setting and heat stable. When forming alginate gels, two contiguous, diaxially linked guloronic residues form a cavity that acts as a binding site for calcium ions "cooperative binding". This behavior, usually described as the "egg-box model", results in the formation of a 3D gel network (Grant, Morris, Rees, & Smith, 1973; Sime, 1990). Although the egg-box model has been amply used it has been questioned several times and is still subject to controversy. Numerous studies have been performed to characterize the mechanisms and structural features involved in the gelation of alginate. These have shown a two-stage process in the mechanism of calcium alginate gelation: first, the formation of strongly linked dimer associations with important contributions from van der Waals and hydrogen bonding interactions, followed by the formation of weaker inter-dimer associations that display no particular specificity, and being mainly governed by electrostatic interactions (Braccini & Pérez, 2001; Morris, Rees, Thom, & Boyd, 1978; Sikorski, Mo, Skjak-Braek, & Stokke, 2007).

Rheological or mechanical properties (MP) of alginate fibers may have a major influence on the acceptance of a product because texture properties of foods are linked to deformation, disintegration and flow under strain. Due to the very rapid and irreversible binding reaction between multivalent cations and alginates, a direct mixing of these two components rarely produces homogeneous gel networks (Draget, 2000, Chap. 22). When the ion (that is, Ca^{2+}) diffuses into a stream of alginate solution, a gel is immediately formed at the interface and MP of alginate fibers are directly related to their chemical structure (Fabra, Talens, & Chiralt, 2010). Values of tensile strength in calcium alginate fibers may depend on intra- or intermolecular associations (Espino-Díaz et al., 2010), indeed, the physical properties of biopolymers depend on whether the molecules are in the disordered or ordered state. In the disordered state, interactions depend mainly on space-occupancy considerations, whereas in the ordered state, molecular interactions create structures capable of stable association into compact networks (Lazaridou, Biliaderis, & Kontogiorgios, 2003). The importance of the G units in the gelation of alginate is highlighted by the fact that the gel strength is a function of the total content and length of contiguous G-blocks as well as the concentration of the cation (Sikorski et al., 2007; Simpson, Stabler, Simpson, Sambanis, & Constantinidis, 2004), whereas changes in frecuency and length of contiguous G units alter the overall strength of the gel (Simpson et al., 2004).

The fracture stress is a measure of the "strength" of a material (Walstra, 2003). This suggests that material fracture takes place when the stress overcomes the cohesive/adhesive forces within the material. For that reason, the fracture stress of alginate gels is proportional to the network crosslink density (Zhang, Daubert, & Foegeding, 2005). The change in density of the gel matrix depends on the concentration either of sodium alginate or calcium salt (Stokke, Draget, Smidsrod, Yuguchi, Urakawa, & Kajiwara, 2000). Contrary to engineering polymers, the mechanical properties (like fracture mechanisms) for many food biopolymer gels are still poorly understood. Despite the wide use of alginate fibers, studies on their MP are limited in the scientific literature.

Hence, the main objective of this research was to produce uniform calcium alginate fibers using a microfluidic device (MFD) and study the effect of concentration of alginate [Alg] and calcium chloride [$CaCl_2$] on their mechanical properties.

2. Materials and methods

2.1. Preparation of sodium alginate and calcium chloride solutions

Solutions of sodium alginate powder Gelymar (Natural Extracts S.A., Chile) used was from *Macrocystis pyrifera* with the following average composition: 16% G [α-L guluronic acid], 38% M [β-D-mannuronic acid] and 46% of MG alternating units (low viscosity, 50–200 cP for a 1% aqueous solution at 20 °C). Sodium alginate at concentrations between 1.25% and 2.5% (until complete dissolution) were prepared. A small amount of red dye (red Laca FC-2030), 0.5% (w/w) was emulsified (by an Ultra Turrax, basic mixer during a two-step, 5 min at 25,000 rpm) into each alginate solution in order to distinguish the fiber at the outlet of the MFD. Finally, solutions were allowed to stand for 24 hours at 4 °C before use. $CaCl_2$ solutions ($CaCl_2{\cdot}2H_2O$ p.a., CA-0520, Heyn, Santiago, Chile) were prepared at different concentrations, % (w/v) based on weight of the anhydrous salt.

2.2. Production of calcium alginate fibers

In Fig. 1, a sketch of the microfluidic device (MFD) used to produce calcium alginate fibers is presented. It was fabricated by combining transparent polycarbonate plates using microfabrication technique and a metal needle. A detailed view of the MFD, to create the coaxial flow, is presented inside the dotted circle in Fig. 1. The metal needle (inner diameter D_{needle} = 0.51 mm) and the polycarbonate capillary tube ($D_{capillary}$ = 3 mm) were co-axially assembled. The $CaCl_2$ solution was injected through the outer capillary whereas the alginate solution was introduced in the inner capillary. Two digital syringe pumps (Model 1000, New Era Pump System Inc., Farmingdale, NY, USA) were employed to produce a controlled flow rate. A fixed alginate flow rate were used, for Q_{Alg} = 1 mL min^{-1} and calcium chloride Q_{CaCl_2} = 5 mL min^{-1}. The calcium alginate fibers moved downward in the vertical laminar flow (this position is important to avoid clogging), while at the interface of both fluids, the Alg solutions met with the polycation (Ca^{2+}) from the $CaCl_2$ solution. A long outlet capillary tube was employed to form the calcium alginate gel on the fiber surface. The polymerized calcium alginate fibers were immediately collected in a beaker that contained 1000 cm^3 of $CaCl_2$ solution to the same concentration that was entered to the MFD.

2.3. Alginate calcium fiber diameter measurements

Measurements of the diameter of single alginate calcium fibers (D_{fiber}) were obtained using a stereo microscope (Olympus SZX7, Optical Co. Ltd., Tokyo, Japan), at magnifications up to 85.5×. Images were recorded with a digital CCD camera Cool Snap Pro Color (Photometrics Roper, Division Inc, Tucson, AZ, USA), processed and analyzed using Image-Pro Plus software (Media Cybernetics, Inc., Silver Spring, MD, USA). Ten samples were measured for each experimental run.

2.4. Moisture content

Moisture content of calcium alginate fibers (about 2–3 g from the container A, Fig. 2) were determined by drying the samples in a convective hot air oven at 105 °C until constant weight and expressed in percentage. Measurement were run in triplicates.

2.5. Mechanical properties measurements

Mechanical properties of calcium alginate fibers [tensile stress at fracture (σ_{max}), tensile strain at fracture or break ($\Delta L/L_0$) and apparent Young's modulus (E)] were measured at room temperature (25 °C) using a Universal Texture Analyser TA.XT2i (Stable Micro Systems, Godalming, Surrey, GU7 1YL, UK) in the tension mode. The calibration was carried out using a 5 kg load cell and initial grip separation was set at 50 mm. The specimen consist of a bundle of parallel, untangled, calcium alginate fibers, that is, a set of 20 fibers (Fig. 2). A constant deformation speed of 0.1 mm/s was

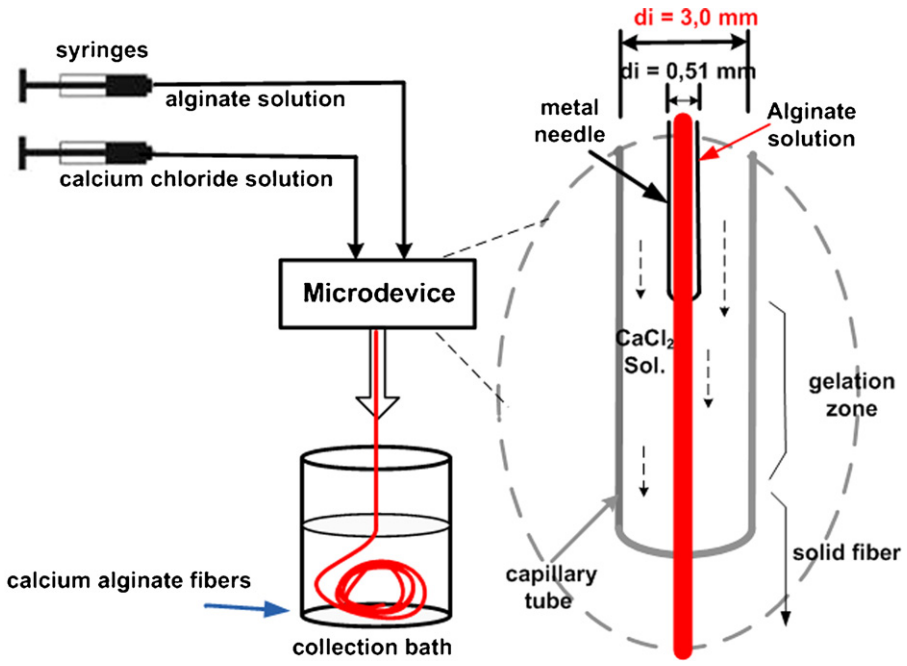

Fig. 1. Sketch of the experimental setup for generating calcium alginate fibers.

applied up to a tension strain beyond the break point. The force versus distance data was recorded for six replicates.

2.6. Experimental design and data analysis

The effect of the independent variables [Alg] and [$CaCl_2$] (in coded or real levels) on dependent variables MO (y_1) and MP [tensile stress at break (y_2), tensile strain at break (y_3) and apparent Young's modulus (y_4)] was studied using response surface (RS) methodology. The selected range of [Alg], between 1.25% and 2.5%, was chosen after performing preliminary experiments so that it was possible to continuously produce calcium alginate fibers with an almost constant diameter. Below the lower limit of [Alg] (<1.25%), we obtained very weak fibers, which did not record data of texture, and above the upper limit (>2.5%) we could not obtain continuous fibers, probably due to the high viscosity of the solutions of sodium alginate, making it difficult to have a continuous flow through the MFD. The coded levels (x) of independent variables were −1, 0 and +1 while the real levels (X_1 for [Alg]) were 1.25%, 1.875% and 2.5% and (X_2 for [$CaCl_2$]), 0.5%, 1.5% and 2.5%.

The experimental values of concentration (%) of sodium alginate solutions used in the experimental design correspond to 11.42, 17.13 and 22.84 mM; and the values that correspond to the calcium chloride solutions (%) are: 45.05, 135.16 and 225.27 mM. The amount of divalent cation, Ca^{2+}, required to react stoichiometrically with G-blocks can be calculated by considering that two guluronic acid units plus one divalent cation are required to create one ionic crosslink (Morris, Rees, Thom, & Boyd, 1978). The stoichiometric amount of Ca^{2+} required to saturate the carboxylates groups of alginate solutions are: 5.71, 8.57 and 11.42 mM. The values of the ratio ($Ca^{2+}{}_{experimental}/Ca^{2+}{}_{stoichiometric}$) vary from 3.9 (for [Alg] = 2.5% or 22.84 mM and [$CaCl_2$] = 0.5% or 45.05 mM) to 39.5 (for [Alg] = 1.25% or 11.42 mM and [$CaCl_2$] = 2.5% or 225.27 mM), and a value of 15.8 for the center point, where [Alg] = 1.875% or 17.13 mM and [$CaCl_2$] = 1.5% or 135.16 mM.

A 3-levels factorial design in 3 blocks which studied the effects of 2 factors ([Alg] and [$CaCl_2$]), was executed twice including an extra centerpoint per block, resulting in 24 runs (Table 1). All experiments were performed randomly and experimental data were analyzed to fit polynomial models as RS using an analysis of variance (ANOVA). Statistical significance was determined using the Statgraphics Plus software (Statistical Graphics Corporation, version 5.1, Rockville, USA), at a probability level of 0.05 ($p < 0.05$). A stepwise procedure was employed to simplify the models and three-dimensional surface plots were generated. The dependent variables were expressed individually as a function (Y) of the aforementioned independent variables (coded or real level of variables) using the following model polynomial Eq. (1):

$$Y = \beta_0 + \beta_1 x_1 + \beta_2 x_2 + \beta_{11} x_1^2 + \beta_{22} x_2^2 + \beta_{12} x_1 x_2 \quad (1)$$

3. Results and discussion

3.1. Effect of residence time on mechanical properties

Residence time was defined as the time during which the alginate fibers bundle remained exposed to the same [$CaCl_2$]. After producing a continuous fiber calcium alginate for about 5 min into the calcium chloride bath, the fiber was cut (Fig. 2), and measuring of residence time began. The residence time in Fig. 2 was the amount of time the fibers remained in the container A and B but the time in the first container was much higher than in the second ($t_A \gg t_B$). The container B was used solely to facilitate handling and formation of the fibers bundle of calcium alginate. Fig. 3 shows that the signatures derived from the mechanical testing of the bundle of fibers with [Alg] = 2% formed in [$CaCl_2$] = 0.5% were similar after a residence time exceeding 30 min. For other combinations of concentrations of the experimental design, the behavior was similar, not observed changes in mechanical properties of fibers after this time, so the tensile stress measurements were conducted at residence times greater than 30 min ($t > 30$ min). During exposure to the $CaCl_2$ bath the gelation interface moves from the surface to the centre of the fiber. As a first approach, the minimum gelation time can be obtained from Fick's second law $\partial C/\partial t = D(\partial^2 C/\partial x^2)$ expression which is possible to approximate as $C/t_{gel} \approx D(C/L^2)$ where L is a characteristic length given by radius of a cylindrical fiber (~200 μm), and D the diffusion coefficient of the calcium chloride in water: 10^{-9} m^2/s (Ribeiro et al., 2008). Thus the minimun gelation

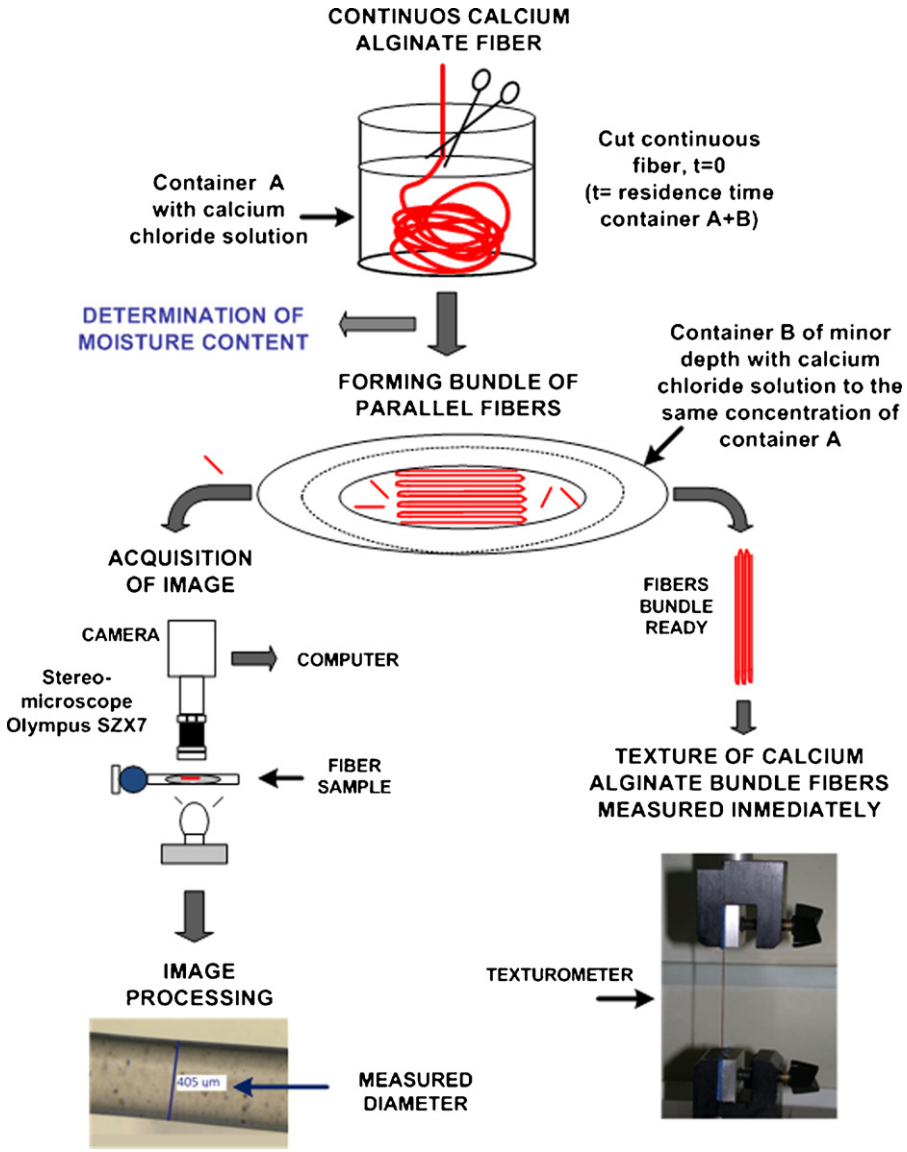

Fig. 2. Procedures showing moisture content, diameter of individual fibers and texture determinations of fiber bundles (total residence time t_{total}, is the sum of the times that the bundle of fibers is in containers A and B, $t_{total} = t_A + t_B$; $t_A \gg t_B$).

time, $t_{gel} \approx L^2/D$ is estimated be close to 40 s. This estimated time to gel was the minimum time that a fiber needs to gel completely assuming that D is constant. However, when the fiber begins to gel, D decreases and t_{gel} increases. The present experimental result was consistent with other reported studies where gelation depends on diffusion of calcium ions through interface or gel membrane that requires times from seconds (Shin et al., 2007) to several hours, e.g., up to 24 h for pieces of 3.2 cm diameter in the case restructured scallops (Roopa & Bhattacharya, 2008; Suklim, Flick, Marcy, Eigel, Haugh, & Granata, 2004).

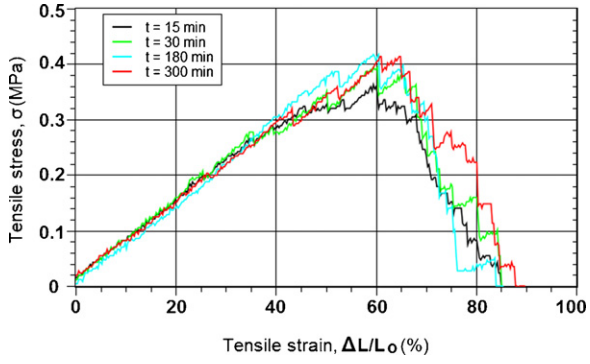

Fig. 3. Signatures of the mechanical test as a function of residence time in the $CaCl_2$ solution. Tensile stress (MPa) vs strain (%) for [Alg] = 2% and [$CaCl_2$] = 0.5%.

3.2. Diameter of fibers

The MFD used to produce alginate fibers was a slightly modified model of that developed by Skurtys and Aguilera (2009) and similar to the one reported by Shin et al. (2007) (Fig. 1). The fibers produced with the MFD had a uniform diameter (10% variation around mean diameter) and showed the advantage of being easily manipulated allowing the formation of fibers bundle (Fig. 2). The procedure for measuring the diameter of individual fibers is as shown in Fig. 2, the mean diameter was used to calculate the cross sectional area of the fibers bundle (Eq. (3)) and this value was used subsequently to calculate the tensile stress. The mean diameter of calcium alginate fibers ranged between 300-550 μm, Table 1.

Table 1
Experimental design in coded and real independent variables (x or X) and observed responses of the dependent variables (y).

Test N°	Sodium Alginate (%)		Calcium Chloride (%)		Diameter[a]	Moisture[a]	Mechanical properties		
	Coded level x_1	Real coded X_1	Coded level x_2	Real coded X_2	D_{fiber}, (μm)	MO (%) y_1	σ_{max} (MPa) Y_2	$\Delta L/L_0$ Y_3	E (MPa) y_4
1	−1.0	1.25	−1.0	0.5	365(26)	96.3(0.3)	0.260	0.372	0.459
2	0.0	1.875	0.0	1.5	461(34)	94.9(0.4)	0.465	0.733	0.540
3	1.0	2.5	1.0	2.5	548(16)	91.1(0.4)	0.354	0.686	0.324
4	0.0	1.875	0.0	1.5	451(41)	94.2(0.5)	0.437	1.052	0.540
5	0.0	1.875	−1.0	0.5	473(21)	94.7(0.2)	0.383	0.811	0.446
6	1.0	2.5	0.0	1.5	539(18)	93.6(0.4)	0.699	0.999	0.408
7	−1.0	1.25	1.0	2.5	301(34)	94.5(0.4)	0.230	0.930	0.171
8	0.0	1.875	0.0	1.5	456(37)	94.0(0.2)	0.424	0.773	0.563
9	1.0	2.5	−1.0	0.5	451(42)	95.4(0.2)	0.510	1.118	0.243
10	−1.0	1.25	0.0	1.5	408(37)	94.6(0.2)	0.330	0.525	0.533
11	0.0	1.875	1.0	2.5	439(32)	92.8(0.3)	0.424	1.143	0.217
12	0.0	1.875	0.0	1.5	461(46)	93.9(0.4)	0.432	1.110	0.485
13	−1.0	1.25	−1.0	0.5	374(27)	96.3(0.3)	0.263	0.370	0.378
14	0.0	1.875	0.0	1.5	455(34)	94.6(0.3)	0.454	0.842	0.498
15	1.0	2.5	1.0	2.5	530(27)	91.9(0.3)	0.362	0.683	0.322
16	0.0	1.875	0.0	1.5	461(39)	94.9(0.4)	0.442	0.843	0.523
17	0.0	1.875	−1.0	0.5	475(23)	95.1(0.3)	0.374	0.859	0.435
18	1.0	2.5	0.0	1.5	545(21)	93.2(0.4)	0.711	1.166	0.390
19	−1.0	1.25	1.0	2.5	292(32)	94.5(0.4)	0.216	0.841	0.186
20	0.0	1.875	0.0	1.5	471(27)	94.6(0.5)	0.444	0.732	0.499
21	1.0	2.5	−1.0	0.5	461(45)	95.3(0.2)	0.509	1.153	0.340
22	−1.0	1.25	0.0	1.5	399(25)	94.7(0.3)	0.339	0.490	0.568
23	0.0	1.875	1.0	2.5	446(34)	92.6(0.3)	0.427	1.148	0.217
24	0.0	1.875	0.0	1.5	436(19)	93.9(0.1)	0.475	0.804	0.508

[a] Average and standard deviation in parentheses for diameter and moisture content.

3.3. Effect of the factors on response surface (RS)

The RS graphs were obtained from the regression equations, keeping the response function on the Z-axis with X- and Y- axes representing the two independent variables related to concentration. The response functions were approximated by a second degree polynomial (Eq. (1)) with linear, quadratic and interaction effects (Table 2).

3.3.1. Moisture content

Fig. 4 shows contour plots of RS for moisture content (MO). The model estimates was statistically significantly ($p < 0.05$; $R^2 = 0.92$) and using the notation of Eq. (1), the best fit of the coded model is:

$$Y_1 = 94.2129 - 0.8408 \cdot x_1 - 1.2908 \cdot x_2 + 0.0938 \cdot x_1^2 - 0.1263 \cdot x_2^2 - 0.6755 \cdot x_1 x_2 \quad (2)$$

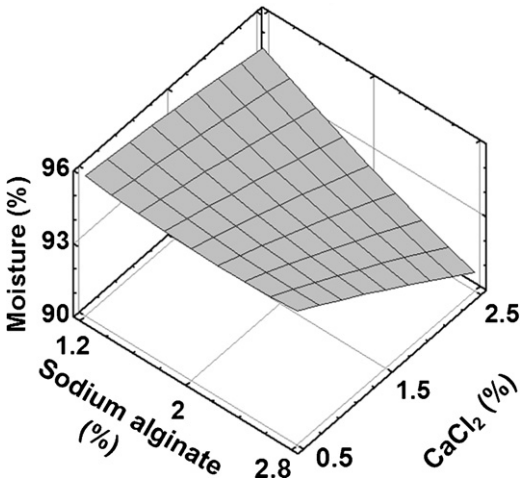

Fig. 4. Response surface for moisture content (MO) as a function of the concentration of sodium alginate and calcium chloride.

Regression coefficients and analysis of variance for MO are shown in Table 2 and maximum and minimum values of model are shown in Table 3. Fig. 4, indicate that MO decreased slightly with an increase in the [Alg] and decreases drastically with increasing the [$CaCl_2$]. Higher values of tensile strain ($\Delta L/L_0 \sim 100\%$ for [Alg] ≥ 1.8%) showed values of MO below 95%. An important variable in MP is the moisture content of calcium alginate fibers, so the presence of a high [$CaCl_2$] could affect the hydration of the alginate fibers showing a drastic decrease in MO. In alginate gels, the swelling rate constant decreases with an increase in the calcium concentration, indicating that the diffusion rate decreases at higher calcium concentrations (Davidovich-Pinhas & Bianco-Peled, 2010). High values in the tensile strain and low values in the tensile stress, could be related to the fact that water acts as plasticizer in fibers and reduces interactions between the adjacent chains in the biopolymers, making them more elastic thereby increasing mobility and flexibility of the fibers. This behavior was also observed in pigskin gelatin films (Bergo & Sobral, 2007).

3.3.2. Maximum tensile stress (σ_{max})

Maximum tensile stress (σ_{max}) was calculated by dividing the maximum force applied (at break) by the original cross-sectional area through which the force is applied (A_{bundle}). The cross-sectional area of the bundle of calcium alginate fiber was estimated from radius of a single fiber, R_{fiber}, multiplied by the number of fibers in the bundle (Eq. 3):

$$A_{bundle} = 20 \cdot \pi \cdot R_{fiber}^2 = \pi \cdot R_{bundle}^2 \quad (3)$$

Contour plots of RS for maximum tensile stress (σ_{max}) are depicted in Fig. 5. Strengthening and weakening of fibers were observed. The tensile stress increases with increasing [$CaCl_2$] up to a maximum around [$CaCl_2$] ≈ 1.41% (Table 3), then values of tensile stress decreased (weakening) as [$CaCl_2$] increased. A similar pattern was observed by Mao, Tang, and Swanson (2000) for 1.5% mixed gellan gels (high acyl to low acyl ratio, 50/50) where a maximum tensile stress of 0.108 MPa was reported. In another study by Zhang et al. (2005) the authors concluded, on the contrary, that the tensile

Table 2
Coefficients of the regression equations for response functions (Y) in coded and real levels of independent variables.

Coefficients polynomial[a]	Coded level of variables				Real level of variables			
	Moisture	Mechanical Properties			Moisture	Mechanical Properties		
	MO (%) Y_1	σ_{max} (MPa) Y_2	$\Delta L/L_0$ Y_3	E (MPa) Y_4	MO (%) Y_1	σ_{max} (MPa) Y_2	$\Delta L/L_0$ Y_3	E (MPa) Y_4
β_0	92.2146	0.4693	0.8870	0.5164	96.5074	−0.0670	2.0956	0.2748
β_1	−0.8667*	0.1257*	0.1896*	−0.0223	−0.9187*	0.1472*	2.2924*	0.1377
β_2	−1.3083*	−0.0237	0.0622	−0.0720*	1.1329*	0.3036	0.6699	0.2666*
β_{11}	0.1313	0.0046	−0.1436*	−0.0352	0.336	0.0119	−0.3677*	−0.0901
β_{22}	−0.0938	−0.1130*	0.0517	−0.1814*	−0.0938	−0.1129*	0.0517	−0.1814*
β_{12}	−0.72*	0.0039	−0.2543*	0.0686*	−1.152*	0.0062	−0.4068*	0.1098*
mae	0.2789	0.0369	0.0935	0.0343	0.2789	0.0369	0.0935	0.0343
R^2	0.92	0.86	0.78	0.89	0.92	0.86	0.78	0.89

mae: the mean absolute error or the average value of the residuals. R^2: the R-squared statistic indicates that the model as fitted explains the % of the variability in the dependent variables.

[a] Polynomial model (coded variables): $Y = \beta_0 + \beta_1 x_1 + \beta_2 x_2 + \beta_{11} x_1^2 + \beta_{22} x_2^2 + \beta_{12} x_1 x_2$. Polynomial model (real variables): similar to above (change coded variables 'x' by real variable 'X'). Values x were −1, 0, and +1 (for both x_1 and x_2). Values X_1 were 1.25%, 1.875%, and 2.5%; values X_2 were 0.5%, 1.5%, and 2.5%. Y_1 = moisture content; Y_2 = tensile stress at break; Y_3 = tensile strain at break; Y_4 = apparent Young's Modulus.

* $p < 0.05$: effects have p-values less than 0.05, indicating that they are significantly different from zero at the 95% confidence level.

Table 3
Maximum and minimum values of the response functions in coded and real levels of independent variables.

Independent variables	MO (%) Y_1	σ_{max} (MPa) Y_2	$\Delta L/L_0$ Y_3	E (MPa) Y_4
Maximum (coded level of variables)				
x_1	−1.00	1.00	1.00	−0.63
x_2	−1.00	−0.09	−1.00	−0.32
Maximum value	95.71	0.60	1.18	0.53
Minimum (coded level of variables)				
x_1	1.00	−1.00	−1.00	−1.00
x_2	1.00	1.00	−1.00	1.00
Minimum value	91.36	0.21	0.29	0.18
Maximum (real level of variables)				
X_1	1.25	2.50	2.50	1.48
X_2	0.5	1.41	0.50	1.18
Maximum value	95.71	0.60	1.18	0.53
Minimum (real level of variables)				
X_1	2.50	1.25	1.25	1.25
X_2	2.50	2.50	0.50	2.50
Minimum value	91.36	0.21	0.29	0.18

stress increased with [$CaCl_2$] or [Alg]. Finally, the model estimating tensile stress was statistically significantly (Table 2) ($p < 0.05$; $R^2 = 0.86$) and using the notation of Eq. (1), the best fit of the coded model was the following (Eq. 4):

$$Y_2 = 0.4693 + 0.1257 \cdot x_1 - 0.0237 \cdot x_2 - 0.0046 \cdot x_1^2 - 0.1130 \cdot x_2^2 + 0.0039 \cdot x_1 x_2 \quad (4)$$

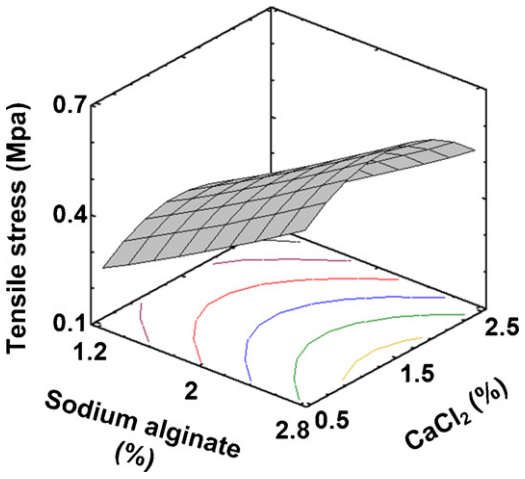

Fig. 5. Response surface for maximum tensile stress (σ_{max}) as a function of the concentration of sodium alginate and calcium chloride.

Regression coefficients and analysis of variance for tensile stress (Y_2) are shown in Table 2 and maximum and minimum values of the model are shown in Table 3. The maximum tensile stress varied between 0.2 and 0.6 MPa.

In practice, the stoichiometric amounts required to saturate the G-blocks of sodium alginate solutions is surpassed several times to reach the highest gel strength (Ca^{2+} = 127 mM or 1.41%), so the number of times of stoichiometric Ca^{2+} required at low concentrations of [Alg] is greater than for high concentrations. Therefore, for a solution of [Alg] = 1.0%, it required about 27 times the concentration of Ca^{2+} stoichiometric requirement, and for a solution of [Alg] = 3.0% required about 9 times.

Numerous studies concluded that the gel strength increases with increasing calcium concentration, since these studies used increasing concentrations of Ca^{2+} source to limit values relatively low (compared to those used in this study), for example up to 30 mM (Stokke et al., 2000), 35 mM (Zhang et al., 2005), 40 mM (Davidovich-Pinhas & Bianco-Peled, 2010). In this work, much higher concentrations (e.g., 225 mM Ca^{2+}) were used that allowed us to observe behavior of the response variables in a wider range [$CaCl_2$].

3.3.3. Tensile strain at break ($\Delta L/L_0$)

Tensile strain at break ($\Delta L/L_0$) was calculated by dividing the elongated distance of the fiber bundle at break by the initial length of the specimen (L_0 = 50 mm). A large tensile strain corresponds to a deformable material. Fig. 6 shows contour plots of RS for tensile

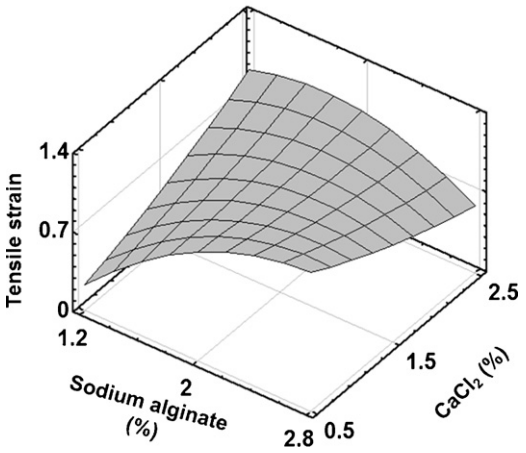

Fig. 6. Response surface for tensile strain ($\Delta L/L_0$) as a function of the concentration of sodium alginate and calcium chloride.

strain ($\Delta L/L_0$) as a function of [Alg] and [$CaCl_2$]. A statistically significant model ($p < 0.05$; $R^2 = 0.78$) was estimated and using the notation of Eq. (1) the best fit coded model was the following (Eq. 5):

$$Y_3 = 0.8870 + 0.1896 \cdot x_1 + 0.0622 \cdot x_2 - 0.1436 \cdot x_1^2 + 0.0517 \cdot x_2^2 - 0.2543 \cdot x_1 x_2 \quad (5)$$

Regression coefficients and analysis of variance for tensile strain at break are shown in Table 2 and values obtained from the model are exhibited in Table 3. The R^2 was <0.80, this could be attributed to the simplification of the model (Eq. (1) and Table 2), but also to experimental conditions (Draget et al., 2006). Fig. 6 shows values of tensile strain for calcium alginate fibers close to 100%, being the maximum value of tensile strain calculated (Table 3) of 1.18 for [Alg] = 2.5% and [$CaCl_2$] = 0.5%. Low tensile stress values showed high values of tensile strain and this may due to the low G residues content of the sample of alginate (16%). Other authors reported that the tensile strain was insensitive to [$CaCl_2$] or [Alg] (Zhang et al., 2005). Moreover, the tensile strain values obtained were higher than those reported in another study (Roopa & Bhattacharya, 2008) for cylindrical samples (40 mm in diameter and 10 mm in height), whose values were between 17.6% and 38.8% ([Alg] = 0.75 and 2.25%, respectively).

3.3.4. Apparent Young's modulus

The apparent Young's modulus of elasticity is defined as the initial slope of the stress–strain curve (before the break point). The apparent Young's modulus (E) was calculated using the slope of the curve between tensile stress and tensile strain (σ vs $\Delta L/L_0$) in the linear viscoelastic range (~15% secant modulus) (Fig. 7a).

Fig. 7b shows contour plots of RS for apparent Young's modulus (E). A statistically significant model ($p < 0.05$; $R^2 = 0.89$) was estimated and using the notation of Eq. (1) the best fit coded model is the following (Eq. 6):

$$Y_4 = 0.5164 - 0.0223 \cdot x_1 - 0.0720 \cdot x_2 - 0.0352 \cdot x_1^2 - 0.1814 \cdot x_2^2 + 0.0686 \cdot x_1 x_2 \quad (6)$$

Regression coefficients and analysis of variance for apparent Young's modulus (coded and real values) are shown in Table 2 and maximum and minimum values of the model are presented in Table 3. This bell-shaped behavior of E (Fig. 7b) as a function of concentration has also been observed in mixed gellan gels when

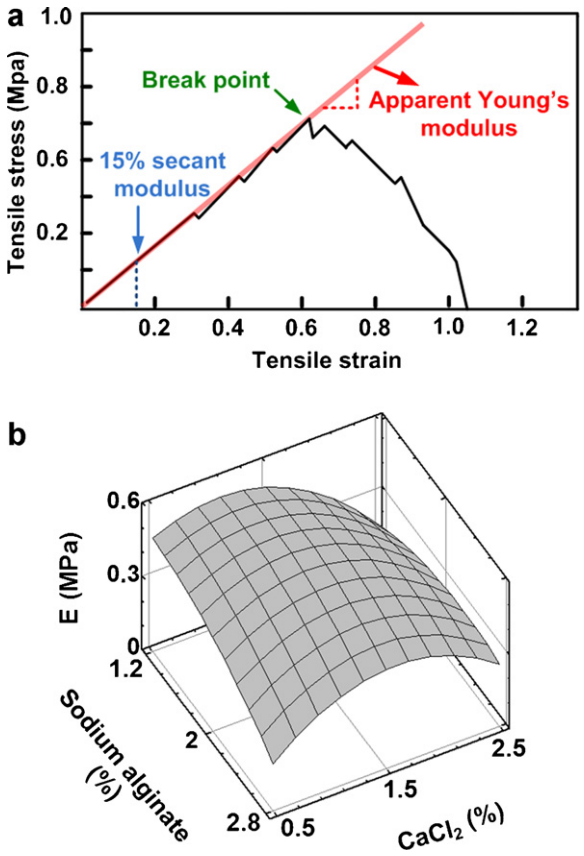

Fig. 7. (a) Apparent Young's modulus (slope of the stress–strain curve before the break point) at 15% secant modulus. (b) Response surface for apparent Young's modulus (E) as a function of the concentration of sodium alginate and calcium chloride.

[$CaCl_2$] increased (Mao et al., 2000). Highest values of apparent Young's modulus reported here are around 0.5 MPa, within the order of magnitude found for gels about 1 MPa (Yada, 2004) but higher than data reported for calcium alginate gels in other studies (Davidovich-Pinhas & Bianco-Peled, 2010; Suklim et al., 2004); however, samples of sodium alginate used has a higher content of G, 30% to 75% (Davidovich-Pinhas & Bianco-Peled, 2010). For foods scientists, the tensile stress at break often correlates better with the mouthfeel of a gel than does the elastic modulus (Draget et al., 2006). Figs. 5, 6 and 7b suggest that food fibers with different mechanical properties may be designed by properly selecting the levels of [$CaCl_2$] and [Alg]. Alginate occurs in the plant as of different metals, primarily sodium and calcium and its biological functions are salts principally of a structural nature (provide flexibility and strength) and as ion exchange species (Craigie, Morris, Rees, & Thom, 1984). The G-blocks have a high affinity for Ca^{2+}, and it is these ions which are mainly responsible for gel strength (Percibal, 1979; Sikorski et al., 2007). In general, the stiffness of the plant reflects the content of G-blocks, as result of their ability to form strong gels by crosslinking with calcium.

According to the results obtained, as the calcium alginate gel reaches its maximum strength, the amount of Ca^{+2} used for inter- and intra-chain associations is higher compared to that stoichiometrically required to saturate the G-blocks. It is possible that Ca^{+2} is not only required to saturate the carboxylates groups, but may also get involved to a lesser extent in Ca^{+2} associations with other components of the alginate. Some studies indicate that Ca^{2+} is also involved in the gelation of the M-blocks; however, the mechanical strength of calcium alginate gels is mainly due to junctions formed by the G-blocks with a strong auto-cooperative binding of Ca^{2+} between the chains in the gel state. The M-blocks and MG-blocks

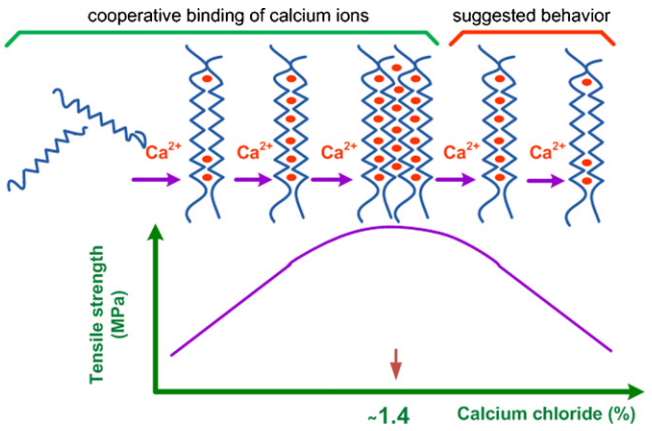

Fig. 8. Scheme suggesting a mechanism that explains the strengthening and weakening of calcium alginate fibers as a function of concentration of calcium chloride.

have much lower selectivity for Ca^{2+} and no autocooperative binding mechanism. Smidsrod (1974) concludes that the modulus of rigidity of gels formed by different cations is directly dependent on their ability to bind to the polyuronides by a cooperative inter-chain binding mechanism.

The results shown in Figs. 5, 6 and 7b indicate that may choose the gel strength tailor-made as a function of the [Alg] and [$CaCl_2$].

3.4. Toward a molecular understanding

In order to explain our experimental results, the effect of [$CaCl_2$] on MP of calcium alginate fibers a sketch was presented in Fig. 8. At low [$CaCl_2$], the Ca^{2+} ions contribute to the formation of junction zones that are assumed to consist of dimeric units or "egg-box dimers" (Vreeker et al., 2008). As a result, the gel is formed and MP are directly related to the number of "egg-box" sites formed and the increase in network crosslink density results in a higher fracture stress (Zhang et al., 2005). In the alginate, gel strength is directly related to the total content of G units and the average length of the G-blocks in the gelling polymer. A saturation point is reached when a maximum number of "egg-box" sites is attained leaving long polymeric chains between them (e.g., coinciding with a maximum tensile stress when [$CaCl_2$] ≈ 1.4%). Davidovich-Pinhas and Bianco-Peled (2010) reported an increase in the number of monomeric units within junction zones of alginate gels at high calcium concentration and suggested an increase lateral chain association which reduced the number of junction zones, thus, leading to a decrease in the modulus. The presence of a maximum value in tensile stress may indicate that an optimum number and size of binding sites in calcium alginate gels is attained. However, the literature is unclear as to whether the increase in modulus is caused by a higher strength of the junction zones or by a large number of them (Draget, 2000, Chap. 22).

Results of this study suggest that the "egg-box" model used to describe ionotropic gelation of alginate only partly explain the relation with microstructural and mechanical properties of the gelled material. According to the egg-box association scheme between G units (Grant et al., 1973), calcium ions induce chain-chain associations forming stable junction zones of dimers and later lateral interactions between dimers (left-hand side in Fig. 8). The decrease in gel strength observed after reaching the maximum force at a [$CaCl_2$] ≈ 1.4% or 127 mM, is a suggestion proposed based on the egg-box model (right-hand side in Fig. 8). The experimental evidence leading to this hypothesis is based on: (1) After the maximum in tensile strength due to interchain association is achieved the system will reverse to the formation of dimers with no association between dimers. As [$CaCl_2$] further increases, Ca^{2+} will only partially fill the G-blocks. Changes in cation concentration can alter the number of alginate strands held together in the "egg-box" model, thus altering the strength of the gel network (Simpson et al., 2004). It was found that the diffusion of calcium ions through the gel network was dependent on the initial concentration of calcium, the ionic strength of the alginate solution, and the size of pores in the gel which is formed (Potter, Balcom, Carpenter, & Hall, 1994). At higher [$CaCl_2$] the ionic strength of the sodium alginate solution may play a definite role in the gelling mechanism. It has been suggested that electrostatic interactions are the main driving force for the observed strengthening effects (Draget et al., 2006). (2) Due to the probable presence of intermolecular hydrophobic interactions that are involved in gelation of G-blocks (Tako & Kohda, 1997), leading to a reduction in connectivity between dimers in neighboring chains. As the size of these assemblies increases, their number decrease, with consequent reduction in connectivity and collapse (tight interchain chelation) (Morris, Rees, Thom, & Boyd, 1978). (3) The reasons for this behavior are not understood, but it appears that G-blocks lose affinity for Ca^{+2}. In this regard, the data register of X-ray diffraction for calcium alginate fibers indicate that the junction zone involves random pairs of polymer chains to form dimers through Ca^{2+} coordination according to the egg-box model and for reasons not fully understood, coordination of the Ca^{2+} cations reduces the ability for lateral packing of the dimers (Sikorski et al., 2007).

4. Conclusions

Calcium alginate fibers of continuous and uniform diameter were successfully produced using a microfluidic device and the mechanical properties were studied in controlled manner. For the sample of alginate used, It was shown that the tensile stress of fibers increased with the Ca^{2+} concentration up to a certain point (calcium chloride concentration around 1.4%) and beyond this value the tensile stress decreased. The presence of a maximum in tensile stress may indicate that a determined number and size of binding sites along the polymeric chains of fibers of calcium alginate is attained, and their mechanical properties are directly related to the number of "egg-box" sites formed.

This value (1.4% or 127 mM Ca^{2+}) is several times the stoichiometric requirement to saturate the polymer carboxylates groups. In order to explain the behaviour of the tensile strength beyond the maximum the "egg-box" model was completed. This suggest that the "egg-box" model used to describe ionotropic gelation of alginate only partly explain the relation with microstructural and mechanical properties of the gelled material. And allows the design and manufacturing of gels of calcium alginate with different mechanical properties by properly selecting the levels of concentration of calcium chloride and sodium alginate.

Acknowledgments

We gratefully acknowledge funding sources CONICYT (Comisión Nacional de Investigación Científica y Tecnológica) and FONDECYT project 1095199. We also appreciate the effort of Dr. Sobukola O. P. of the University of Agriculture Abeokuta, Nigeria, in the valuable discussions.

References

Belitz, H.-D., Grosch, W., & Schieberle, P. (Eds.). (2004). *Food Chemistry*. Berlin: Springer.

Bergo, P., & Sobral, P. J. A. (2007). Effects of plasticizer on physical properties of pigskin gelatin films. *Food Hydrocolloids*, *21*(8), 1285–1289.

Bhattarai, N., Li, Z., Edmondson, D., & Zhang, M. (2006). Alginate-based nanofibrous scaffolds: Structural, mechanical and biological properties. *Advanced Materials*, *18*, 1463–1467.

Braccini, I., & Pérez, S. (2001). Molecular basis of Ca^{2+}-induced gelation in alginates and pectins: The egg-box model revisited. *Biomacromolecules*, *2*(4), 1089–1096.
Craigie, J. S., Morris, E. R., Rees, D. A., & Thom, D. (1984). Alginate block structure in phaeophyceae from Nova Scotia: Variation with species, environment and tissue-type. *Carbohydrate Polymers*, *4*(4), 237–252.
Davidovich-Pinhas, M., & Bianco-Peled, H. (2010). A quantitative analysis of alginate swelling. *Carbohydrate Polymers*, *79*(4), 1020–1027.
Draget, K. (2000). Alginates. In G. O. Phillips, & P. A. Williams (Eds.), *Handbook of Hydrocolloids*. Woodhead Publishing Limited: Cambridge England.
Draget, K., Moe, S., Skjak-Braek, G., & Smidsrod, O. (2006). Alginates. In A. M. Stephen, G. O. Phillips, & P. A. Williams (Eds.), *Food Polysaccharides and Their Applications*. CRC Press-Taylor and FrancisGroup.
Espino-Díaz, M., Ornelas-Paz, J. D. J., Martínez-Téllez, M. A., Santillán, C., Barbosa-Cánovas, G. V., Zamudio-Flores, P. B., & Olivas, G. I. (2010). Development and characterization of edible films based on mucilage of opuntia ficus-indica(L.). *Journal of food science*, *75*(6), E347–E352.
Fabra, M. J., Talens, P., & Chiralt, A. (2010). Influence of calcium on tensile, optical and water vapour permeability properties of sodium caseinate edible films. *Journal of Food Engineering*, *96*, 356–364.
Fan, L., Du, Y., Huan, R., Wang, Q., Wang, X., & Zhang, L. (2005). Preparation and characterization of alginate/gelatin blend fibers. *Journal of Applied Polymer Science*, *96*, 1625–1629.
Grant, G. T., Morris, E. R., Rees, D. A., & Smith, P. J. C. (1973). Biological interactions between polysaccharides and divalent cations: The egg-box model. *FEBS Letters*, *32*, 195–198.
Lazaridou, A., Biliaderis, C. D., & Kontogiorgios, V. (2003). Molecular weight effects on solution rheology of pollulan and mechanical properties of its films. *Carbohydrate Polymers*, *52*, 151–166.
Mao, R., Tang, J., & Swanson, B. G. (2000). Texture properties of high and low acyl mixed gellan gels. *Carbohydrate Polymers*, *41*(4), 331–338.
Mikolajczyk, T., & Wolowska-Czapnik, D. (2005). Multifunctional alginates fibres with anti-bacterial properties. *Fibres & Textiles in Eastern Europe Industrial Engineering Chemistry Research*, *13*(3(51)), 35–40.
Moon, S., Ryu, B.-Y., Choi, J., Jo, B., & Farris, R. J. (2009). The morphology ad mechanical properties of sodium alginate based electrospun poly(ethylene oxide) nanofibers. *Polymer Engineering and Science*, *49*, 52–59.
Morris, E. R., Rees, D. A., Thom, D., & Boyd, J. (1978). Chiroptical and stoichiometric evidence of a specific, primary dimerisation process in alginate gelation. *Carbohydrate Research*, *66*(1), 145–154.
Percibal, E. (1979). The polysaccharides of green, red and brown seaweeds: Their basic structure, biosynthesis and function. *British Phycological Journal*, *14*(2), 113–117.
Potter, K., Balcom, B. J., Carpenter, T. A., & Hall, L. D. (1994). The gelation of sodium alginate with calcium ions studied by magnetic resonance imaging (MRI). *Carbohydrate Research*, *257*(1), 117–126.
Ribeiro, A. C. F., Barros, M. C. F., Teles, A. S. N., Valente, A. J. M., Lobo, V. M. M., Sobral, A. J. F. N., & Esteso, M. A. (2008). Diffusion coefficients and electrical conductivities for calcium chloride aqueous solutions at 298.15 K and 310.15 K. *Electrochimica Acta*, *54*(2), 192–196.
Roopa, B. S., & Bhattacharya, S. (2008). Alginate gels: I. Characterization of textural attributes. *Journal of Food Engineering*, *85*(1), 123–131.
Shin, S.-J., Park, J.-Y., Lee, J.-Y., Park, H., Park, Y.-D., Lee, K.-B., Whang, C.-M., & Lee, S.-H. (2007). On the fly continuous generation of alginate fibers using a microfluidic device. *Langmuir*, *23*, 9104–9108.
Sikorski, P., Mo, F., Skjak-Braek, G., & Stokke, B. T. (2007). Evidence for egg-box-compatible interactions in calciumâˆ'alginate gels from fiber X-ray diffraction. *Biomacromolecules*, *8*(7), 2098–2103.
Sime, W. J. (1990). *Food gels*. London/New York: Elsevier Applied Science.
Simpson, N. E., Stabler, C. L., Simpson, C. P., Sambanis, A., & Constantinidis, I. (2004). The role of the $CaCl_2$-guluronic acid interaction on alginate encapsulated BTC3 cells. *Biomaterials*, *25*(13), 2603–2610.
Skurtys, O., & Aguilera, J. M. (2008a). Applications of microfluidic devices in food engineering. *Food Biophysics*, *3*, 1–15.
Skurtys, O., & Aguilera, J. M. (2008b). Structuring bubbles and foams in gelatine solutions within a circular microchannel device. *Journal of Colloid and Interface Science*, *318*, 380–388.
Skurtys, O., & Aguilera, J. M. (2009). Formation of O/W macroemulsions with a circular microfluidic device using saponin and potato starch. *Food Hydrocolloids*, *23*(7), 1810–1817.
Skurtys, O., Bouchon, P., & Aguilera, J. M. (2008). Formation of bubbles and foams in gelatine solutions within a vertical glass tube. *Food Hydrocolloids*, *22*, 706–714.
Smidsrod, O. (1974). Molecular basis for some physical properties of alginates in the gel stat. *Faraday Discussion Chemical Society*, *57*, 263–274.
Stokke, B. T., Draget, K. I., Smidsrod, O., Yuguchi, Y., Urakawa, H., & Kajiwara, K. (2000). Small-angle X-ray scattering and rheological characterization of alginate gels. 1. Ca–Alginate gels. *Macromolecules*, *33*, 1853–1863.
Suklim, K., Flick, G. J., Marcy, J. E., Eigel, W. N., Haugh, C. G., & Granata, L. A. (2004). Effect of cold-set binders: Alginates and microbial transglutaminase on the physical properties of restructured scallops. *Journal of Texture Studies*, *35*, 634–642.
Tako, M., & Kohda, Y. (1997). Calcium induced association characteristics of alginate. *Journal of Applied Glycoscience*, *44*(2), 153–159.
Tonnesen, H. H., & Karlsen, J. (2002). Alginate in drug delivery systems. *Drug development and industrial Pharmacy*, *28*(6), 621–630.
van der Goot, A., Peifhambardoust, S., Akkermans, C., & van Oosten-Manski, J. (2008). Creating novel structures in food materials: The role of well-defined shear flow. *Food Biophysics*, *3*, 120–125.
Vreeker, R., Li, L., Fang, Y., Appelqvist, I., & Mendes, E. (2008). Drying and rehydratation of calcium alginate gels. *Food Biophysics*, *3*, 361–369.
Walstra, P. (2003). Soft solids. In *Physical Chemistry of Foods*. Marcel Dekker: New York Basel., p. 683.
Wang, C., Liu, H., Gao, Q., Liu, X., & Tong, Z. (2008). Alginate–calcium carbonate porous microparticle hybrid hydrogels with versatile drug loading capabilities and variable mechanical strengths. *Carbohydrate Polymers*, *71*(3), 476–480.
Yada, R. Y. (2004). *Proteins in Food Processing*. Cambridge: CRC Woodhead Publishing Limited.
Zhang, J., Daubert, C. R., & Foegeding, E. A. (2005). Fracture analysis of alginate gels. *Journal of food science*, *70*(7), E425–E431.